Available online at www.sciencedirect.com
ScienceDirect
Catalysis Today 122 (2007) 226–232
CATALYSIS TODAY
www.elsevier.com/locate/cattod

Structural and chemical promoter effects of alkali (earth) and cerium oxides in CO oxidation on supported gold

Andreea C. Gluhoi *, Bernard E. Nieuwenhuys

Department of Heterogeneous Catalysis and Surface Chemistry, Leiden Institute of Chemistry, Leiden University, P.O. Box 9502, 2300 RA Leiden, The Netherlands

Available online 26 March 2007

Abstract

Nanostructured Au/Al_2O_3 catalysts prepared by deposition–precipitation with urea were characterized by X-ray diffraction (XRD) and high-resolution transmission electron microscopy (HRTEM) and tested for low temperature CO oxidation. The paper is focused on the effect of two different kinds of additives on the structure and reactivity of Au/Al_2O_3 for CO oxidation: (1) alkali (earth) metal oxides and (2) ceria. The structural properties of nanosized Au particles are drastically affected by the presence of additives. The main role of the alkali (earth) metal oxides is to stabilize the small Au particles against sintering, such that when BaO is added to Au/Al_2O_3, full CO conversion is already achieved at room temperature. For this reaction ceria addition does not result in a higher activity. However, when both BaO and CeO_x are added to Au/Al_2O_3, the catalytic performance of the multicomponent catalyst resembles that of $Au/BaO/Al_2O_3$.

Keywords: Gold; Additives; Alkali (earth) metal oxides; Ceria; Promoters; CO oxidation

1. Introduction

Because of its well-known nobility, gold is inactive in its massive form. However, gold nano-particles exhibit high catalytic activity for CO oxidation even at sub-ambient temperatures [1]. In 1987 Haruta et al. showed that gold-based catalysts may exhibit an extremely high activity if the catalysts are prepared according to specific recipes [1]. Since then a lot of research has been carried out and it is generally accepted that the property of catalytically active gold is related to the presence of discrete, nano-scale gold particles in a very narrow size range 2–5 nm [2–5]. For extensive reviews on this topic we refer to [3,5–15].

In spite of the large number of papers focused on understanding of gold catalysis, the nature of the active sites is still a matter of debate, in particular for CO oxidation, the most frequently studied reaction over these catalytic systems. For some systems it is clear that the size of the Au crystallites is not sufficient to explain the high activity. Therefore, it has been proposed that the perimeter or gold–support interface [16–21], or small Au clusters that have nonmetallic electronic properties due to a quantum-size effect [4], or step sites on the surface and strain defects [22] are more important than only Au nano-particles with a size between 2 and 5 nm. On the other hand, other groups are convinced that cationic gold is responsible for the high activity in CO oxidation [23]. It was also proposed that the activity in CO oxidation is due to an ensemble of metallic Au atoms and Au cations with hydroxyl ligands [7,24]. Alternatively, anionic gold, Au^- was also suggested as active site. These species may be formed if Au is deposited on a defect-rich support, i.e., with an increased concentration of F-centres [25–28].

This paper presents a study concerning the effect of various additives such as alkali (earth) metal oxides and ceria on the structure and reactivity of Au/Al_2O_3 for CO oxidation. It was reported that Au supported on $Mg(OH)_2$ or $Be(OH)_2$ displays a high catalytic activity in CO oxidation, especially if the average size of the Au particles is around 2 nm [29]. A beneficial effect of addition of various alkali (earth) metal oxides, such as Li_2O, Rb_2O, MgO and BaO to Au/Al_2O_3 for oxidation of (un)saturated hydrocarbons [30,31], CO [32], ammonia [33] and reduction of N_2O [34] has already been reported by our group. We have also reported that transition metal oxides and

* Corresponding author.
E-mail address: gluhoi@chem.leidenuniv.nl (A.C. Gluhoi).

0920-5861/$ – see front matter © 2007 Elsevier B.V. All rights reserved.
doi:10.1016/j.cattod.2007.01.066

ceria are extremely efficient promoters for Au/Al_2O_3 in total oxidation of C_3H_6 [35].

2. Experimental

2.1. Catalyst preparation

The unpromoted Au/Al_2O_3 catalyst (5 wt.% Au) was prepared via HDP with urea, using $HAuCl_4{\cdot}3H_2O$ (Aldrich, 99.99%) as the gold precursor. Details concerning the preparation procedures have already been reported [31,35]. Prior to the reaction test all the catalysts have been calcined in pure O_2 at 300 °C for 2 h.

The mixed supports in the form of MO_x/Al_2O_3 (M: Li, Rb, Ba, Ce) or $MO_x/CeO_x/Al_2O_3$ (M: Li, Rb, Ba) were obtained by pore volume impregnation of γ-Al_2O_3 (Engelhard Al-4172P, $S_{BET} = 275\ m^2\ g^{-1}$) with a solution of the corresponding nitrates. A detailed description of the experimental procedure is found in [31]. Au (5 wt.%) was deposited onto MO_x/Al_2O_3 (M/Al = 1/15, atomic ratio) or $MO_x/CeO_x/Al_2O_3$ (M/Ce/Al = 1/1/15, atomic ratio) by HDP with urea. The influence of the Li_2O loading on the catalytic activity of Au/Al_2O_3 was also studied and three $Au/Li_2O/Al_2O_3$ catalysts with different Li/Al ratios, i.e., 1/1, 1/5 and 1/30 have been prepared (all catalysts were 5 wt.% Au). These catalysts will be designated as $Au/Li_2O/Al_2O_3$_X, where X = 1, 5 or 30.

2.2. Catalyst characterization

The extent of gold deposition on the support was determined by means of atomic absorption spectroscopy (AAS).

BET surface areas of the catalysts were measured by N_2 physisorption at −196 °C using an automatic Qsurf M1 analyzer (Thermo Finnigan) [35].

XRD measurements for the fresh and spent (i.e., after catalytic test) catalysts were carried out using a Philips Goniometer (PW 1050/25) diffractometer equipped with a PW Cu 2103/00 X-ray tube operated at 50 kV and 40 mA. The average gold particle size was estimated from XRD line broadening by using the Scherrer equation.

HRTEM measurements were performed using a JEOL 2010 microscope with a point-to-point resolution better than 0.2 nm [35].

All the results related to the physico-chemical properties of the catalysts are summarized in Table 1. In addition, where possible, the metallic surface area of Au was estimated based on the XRD or HRTEM results [32,36]. The HRTEM results have been also used to estimate the Au dispersion.

2.3. Catalytic activity measurements

CO oxidation was carried out in a lab-scale fixed bed reactor in which typically 0.2 g of catalyst was loaded. The activation procedure consisted of in situ heating the catalyst up to 300 °C (1 h), under H_2 flow. The feed gases were controlled by mass flow controllers (Bronkhorst) and set to a total flow of 40 ml min^{-1}, which corresponds to a GHSV ∼2500 h^{-1}. Diluted CO and O_2 (4 vol%/He) were used to study the oxidation of CO and the reactant ratio was $CO/O_2 = 2/1$. The outlet gas concentration was analysed by a gas chromatograph (*Chrompack CP-2002*) equipped with two columns: a Molsieve 5 Å column for detection of CO and O_2 and a Hayesep A column for CO_2 detection.

The reactant mixture was stabilized for at least 30 min at room temperature. Afterwards at least two consecutive heating–cooling reaction cycles were performed. To compare the catalytic performance, the results of the second heating cycle are considered. Third and additional heating–cooling cycles gave almost similar results as those of the second cycle. The specific reaction rate, *r*, expressed as the number of CO (moles) transformed over the amount of Au (mol)/s was also determined.

After performing the test reaction, the catalysts were again analysed by XRD.

3. Results

3.1. Catalyst characterization

The average Au particle size as determined by XRD varies between 4.3 nm, for unpromoted Au/Al_2O_3 and very small,

Table 1
Catalyst characterization by means of AAS, BET, XRD and HRTEM

Catalyst	Au (wt.%)	S_{BET} ($m^2\ g^{-1}$)	d^a_{Au} (nm)	S^a_{Au} ($m^2\ g^{-1}$)	d^b_{Au} (nm)	S^b_{Au} ($m^2\ g^{-1}$)	D_{Au} (%)
Al_2O_3	_	275 ± 5	_	_	_	_	_
Au/Al_2O_3	4.1 ± 0.1	260 ± 5	4.3 ± 0.1	2.4 ± 0.1	5.2 ± 0.3	1.5 ± 0.3	11.5 ± 1.1
$Au/Li_2O/Al_2O_3$	4.0 ± 0.3	278 ± 7	3.2 ± 0.1	3.0 ± 0.1	3.0 ± 0.1	2.5 ± 0.1	19.0 ± 1.0
$Au/Rb_2O/Al_2O_3$	3.5 ± 0.1	294 ± 3	<3.0	_	2.6 ± 0.3	3.6 ± 0.3	33.0 ± 1.1
$Au/BaO/Al_2O_3$	3.6 ± 0.2	240 ± 8	<3.0	_	1.5 ± 0.2	6.2 ± 0.02	55.0 ± 1.2
$Au/Li_2O/Al_2O_3$_1	4.5 ± 0.1	261 ± 5	3.0 ± 0.1	3.8 ± 0.1	n.m.	_	_
$Au/Li_2O/Al_2O_3$_5	4.1 ± 0.2	253 ± 4	4.1 ± 0.2	2.6 ± 0.2	n.m.	_	_
$Au/Li_2O/Al_2O_3$_30	4.2 ± 0.1	269 ± 7	<3.0	_	n.m.	_	_
$Au/CeO_x/Al_2O_3$	4.5 ± 0.1	218 ± 11	<3.0	_	1.7 ± 0.2	7.1 ± 0.2	52.0 ± 1.3
$Au/Li_2O/CeO_x/Al_2O_3$	4.6 ± 0.2	262 ± 10	<3.0	_	2.9 ± 0.1	3.8 ± 0.1	27.0 ± 5
$Au/Rb_2O/CeO_x/Al_2O_3$	4.5 ± 0.3	275 ± 7	<3.0	_	2.8 ± 0.2	2.6 ± 0.2	20.0 ± 4
$Au/BaO/CeO_x/Al_2O_3$	4.4 ± 0.2	259 ± 7	<3.0	_	3.3 ± 0.1	3.0 ± 0.1	23.0 ± 5

d^a_{Au}, mean diameter of gold particles, XRD, fresh catalysts (nm); d^b_{Au}, mean diameter of gold particles, HRTEM, fresh catalysts (nm); S^a_{Au}, gold surface area, XRD ($m^2\ g^{-1}$); S^b_{Au}, gold surface area, HRTEM ($m^2\ g^{-1}$); D_{Au}, gold dispersion, HRTEM; n.m., not measured.

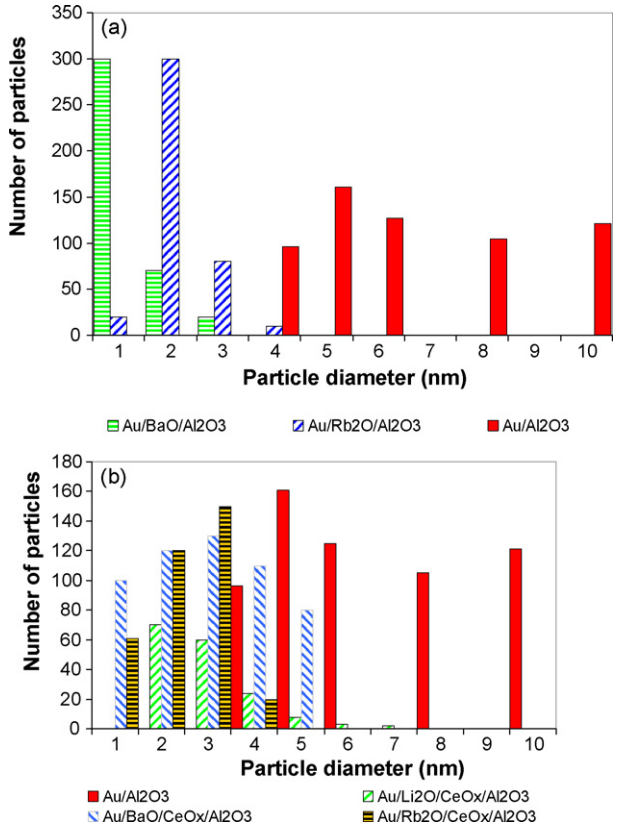

Fig. 1. (a) Particle size distribution as determined by HRTEM for Au/Al_2O_3, $Au/Rb_2O/Al_2O_3$ and $Au/BaO/Al_2O_3$. (b) Particle size distribution as determined by HRTEM for Au/Al_2O_3, $Au/Rb_2O/CeO_x/Al_2O_3$, $Au/Li_2O/CeO_x/Al_2O_3$ and $Au/BaO/CeO_x/Al_2O_3$.

below the detection limit of XRD, when various additives are used. The metallic Au surface area (XRD) varies between 2.4 $m^2\ g^{-1}$ (Au/Al_2O_3) and 3.8 $m^2\ g^{-1}$ ($Au/Li_2O/Al_2O_3$_1).

The Au particle size distribution (HRTEM) of Au/Al_2O_3, $Au/Rb_2O/Al_2O_3$ and $Au/BaO/Al_2O_3$ is presented in Fig. 1a. There is a significant difference concerning the particle size distribution of the samples with or without additive. The growth of the large gold particles at the expense of the smaller Au crystallites found for Au/Al_2O_3 is prevented in the presence of alkali (earth) metal oxides. Fig. 1b compares the particle size distribution for the multicomponent (i.e., with two additives) Au-based catalysts.

The HRTEM micrographs of $Au/CeO_x/Al_2O_3$ and $Au/BaO/CeO_x/Al_2O_3$ catalysts are presented in Fig. 2a and b. The measured lattice spacing of 2.76° A corresponds to the Au (1 1 1) reflection (Fig. 2a).

Based on the HRTEM data, the largest Au dispersion was found for $Au/BaO/Al_2O_3$, 55%.

3.2. Catalytic activity measurements

All the data concerning the catalytic performance of Au-based catalysts are summarized in Table 2. The data include the temperature required for 95% CO conversion, the CO conversion at 70 °C (X_{70}), the specific reaction rate r calculated at 70 °C and the average gold particle size after (d^b_{Au}) reaction

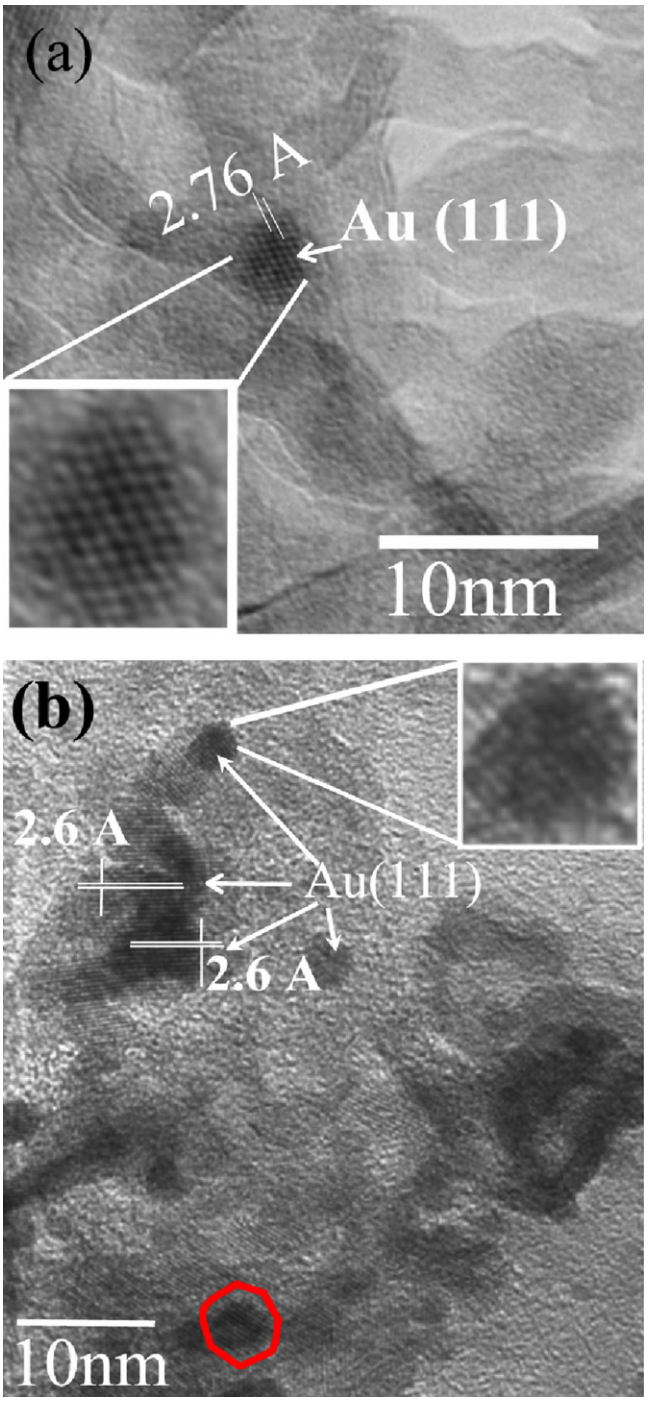

Fig. 2. (a) HRTEM image of $Au/CeO_x/Al_2O_3$. (b) HRTEM image of $Au/BaO/CeO_x/Al_2O_3$.

(XRD). The bare supports showed extremely low catalytic activity under these reaction conditions.

Fig. 3a shows the conversion of CO versus temperature over Au-based catalysts with one single metal oxide as additive, while Fig. 3b depicts the catalytic performance of the multicomponent Au-based catalysts (two additives).

According to Fig. 3a and Table 2, the best performance is obtained for Au combined with BaO and full CO conversion is reached at room temperature. The catalytic activity of

Table 2
$T_{95\%}$, the conversion at 70 °C (X_{70}), the specific reaction rate, r, the average size of the gold particles for the spent (d^{b}_{Au}) Au-based catalysts (XRD)

Catalyst	d^{b}_{Au} (nm)	$T_{95\%}$ (°C)	X_{70}	$r \times 10^3$ (mol CO mol^{-1} Au s^{-1})
Au/Al_2O_3	3.0 ± 0.2	112	0.78	5.5 ± 0.1
$Au/Li_2O/Al_2O_3$	3.2 ± 0.1	89	0.87	6.9 ± 0.1
$Au/Rb_2O/Al_2O_3$	<3.0	78	0.92	8.9 ± 0.1
$Au/BaO/Al_2O_3$	<3.0	<25	1	7.6 ± 0.1[a]
$Au/Li_2O/Al_2O_3$_1	3.1 ± 0.3	123	0.8	4.9 ± 0.1
$Au/Li_2O/Al_2O_3$_5	4.7 ± 0.3	90	0.88	7.2 ± 0.2
$Au/Li_2O/Al_2O_3$_30	3.0 ± 0.1	77	0.93	7.4 ± 0.1
$Au/CeO_x/Al_2O_3$	3.5 ± 0.2	145	0.43	5.0 ± 0.2
$Au/Li_2O/CeO_x/Al_2O_3$	<3.0	100	0.85	8.0 ± 0.1
$Au/Rb_2O/CeO_x/Al_2O_3$	3.3 ± 0.1	152	0.63	5.7 ± 0.1
$Au/BaO/CeO_x/Al_2O_3$	<3.0	<25	1	8.1 ± 0.2[a]

[a] This value corresponds to 100% CO conversion.

Au/Al_2O_3 is also enhanced in the presence of Rb_2O and Li_2O. The loading of Li_2O influences both the size of the Au particles and the catalytic performance of Au/Al_2O_3. The best result is obtained for an atomic ratio Li:Al = 1:30 (1 wt.% Li_2O). A larger amount of Li_2O (atomic ratio Li:Al = 1:1) causes only a small increase in the catalytic performance. In fact, the catalyst with the highest Li_2O concentration shows a lower r compared with the unpromoted Au/Al_2O_3. In spite of its slightly lower r-value, $Au/BaO/Al_2O_3$ shows the lowest $T_{95\%}$.

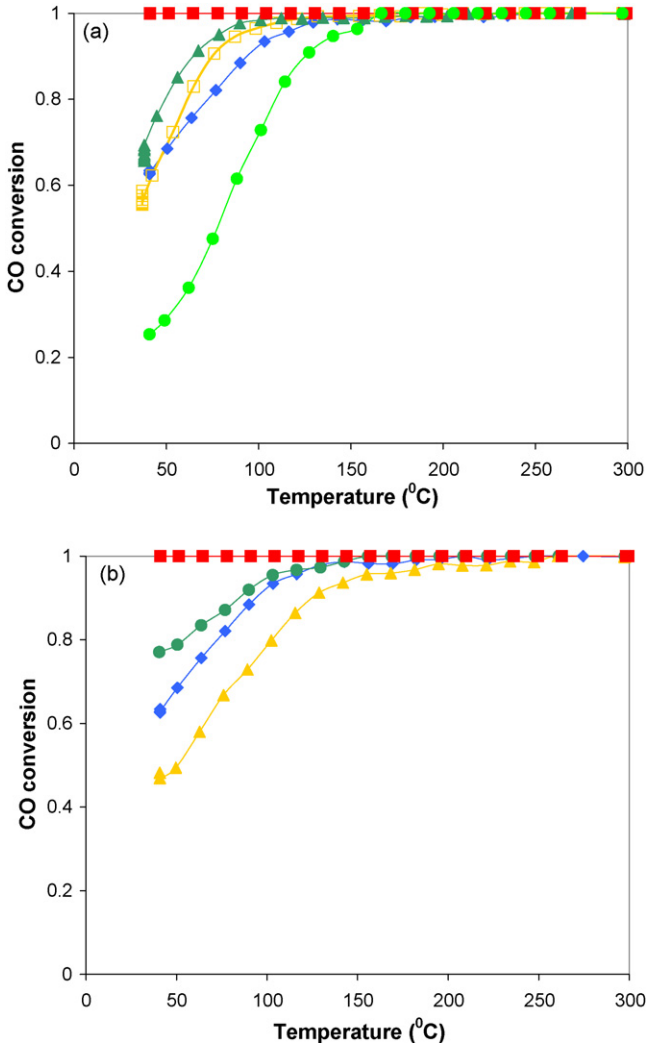

Fig. 3. (a) CO conversion vs. temperature over $Au/BaO/Al_2O_3$ (■), $Au/Rb_2O/Al_2O_3$ (▲), $Au/Li_2O/Al_2O_3$ (□), Au/Al_2O_3 (◆) and $Au/CeO_x/Al_2O_3$ (●). (b) CO conversion vs. temperature over $Au/BaO/CeO_x/Al_2O_3$ (■), $Au/Li_2O/CeO_x/Al_2O_3$ (●), $Au/Rb_2O/CeO_x/Al_2O_3$ (▲), Au/Al_2O_3 (◆).

Albeit the promoting effect of ceria for many oxidation reactions is well-known [37], its addition to Au/Al_2O_3 was rather detrimental for CO oxidation. Possible explanations for this finding will be provided in the next section. However, CeO_x may act as an oxygen supplier during CO oxidation (see below), which makes the combination Au–CeO_x interesting from a practical point of view (i.e., automotive catalysis).

The results presented in Fig. 3b and Table 2 illustrate the result of combining $BaO/Li_2O/Rb_2O$ and CeO_x. Although ceria alone has a rather detrimental effect when added to Au/Al_2O_3, the multicomponent $Au/BaO/CeO_x/Al_2O_3$ is still highly active in CO oxidation and full conversion of CO is reached already at room temperature. High catalytic activity is also shown by $Au/Li_2O/CeO_x/Al_2O_3$.

4. Discussion

It is generally accepted that CO adsorption takes place on Au [38,39] and at the Au–support interface [40,41]. Moreover, based on DFT calculations and surface science studies, it was reported that the availability of many low-coordinated Au atoms, with an increased number of steps and kinks is most important to obtain an active Au-based catalyst [22,42–44].

Taking into account these models, the main issue remains the activation of oxygen. DFT calculations showed that O_2 can adsorb at the Au–support interface, but the dissociation of O_2 on gold cannot occur at low temperatures [45]. It was proposed that the reaction occurs on Au steps via a two-step mechanism involving reaction between CO adsorbed on Au defects and O_2 accommodated at the Au–support interface [45]. In addition, it is possible that the support material induces strain in the gold particles due to the mismatch of the lattice at the interface, an effect that is more pronounced in small gold particles than in larger ones [22].

The results presented throughout this paper show that the catalytic performance of Au/Al_2O_3 is improved by using alkali (earth) metal oxides as additives. The detailed study concerning

the promoter effect of Li_2O revealed that the catalytic performance of Au-based catalysts is influenced by the concentration of Li_2O. Although there is a clear effect of the additives on the size of the gold particles, which, in turn, influences the Au surface area (i.e., active sites), a direct correlation between the size and the catalytic activity could not be established. For example $Au/Li_2O/Al_2O_3$_1 shows the largest metallic surface area, according to the HRTEM results, but the catalytic activity in CO oxidation is not the highest one. Most probably the beneficial effect of this kind of additives can be attributed to a change of the morphology and size of the Au particles. It should be mentioned, however, that our previously reported results obtained by using TPR, DR-UV/vis and XPS did not reveal the presence of ionic gold as a result of alkali (earth) metal oxide addition [32,36].

In our opinion the high activity of gold nano-particles is connected with a relatively high abundance of low-coordinated Au atoms that may be responsible for the high activity [42–44]. For oxidation of (un)saturated hydrocarbons we have shown that this kind of additives are very efficient structural promoters and possibly also help in O_2 activation [30,31]. An earlier study showed that the presence of some alkali (Li, Na, K) metal oxides is beneficial for the catalytic activity of Au/MnO_x and it was hypothesized that this promotion might be connected with the suppression of CO_2 retention [46]. Using FTIR it was found that when MO_x (M: Mg, Mn, and Fe) is added to Au/Al_2O_3, both the C–O stretching frequency and the CO adsorption capacity are significantly affected (decreased) [18]. However, according to that study, MgO induced the smallest effect on the adsorption capacity of Au/Al_2O_3, compared with MnO_x and FeO_x.

Opposite to previous findings [35], that CeO_x can act as an effective promoter for Au/Al_2O_3 in propene oxidation, the present study did not show a promoting effect for CO oxidation. In literature different effects of ceria have been reported. Ceria has been reported either not to be a suitable support for gold-based catalyst in CO oxidation at low temperature [6,47], or extremely active and 50% CO conversion was reached at $T = 250$ K [48]. The authors ascribed the result to Au^+ species. It was also claimed that the morphology of ceria might be even more important than the size of the Au particles [49]. Also the ratio $CO:O_2$ may play an important role, since all the results that reported Au/CeO_2 being active are based on measurements in a large excess of oxygen. It was suggested that the active oxygen may originate from ceria, rather than from the gas phase, and smaller ceria crystallites supply more active O than larger crystallites. The average size of the ceria crystallites for the $Au/CeO_x/Al_2O_3$ presented in Fig. 3a is around 9 nm (XRD) and increases to 10 nm after CO oxidation. Hence, the size of ceria particles is much larger than those reported in [49], i.e., 3.3 nm. This may explain the lower activity of our $Au/CeO_x/Al_2O_3$.

We have already been reported that that CeO_x- and MnO_x-containing Au/Al_2O_3 catalysts are able to convert C_3H_6 to CO_2 in the absence of O_2 in the gas stream [35]. Most probably the reaction mechanism is of the Mars and van Krevelen type.

When a reactant mixture of CO (8.6 ml min^{-1}, 4 vol%CO/He) and Ar was passed over Au/Al_2O_3, $Au/CeO_x/Al_2O_3$ and their

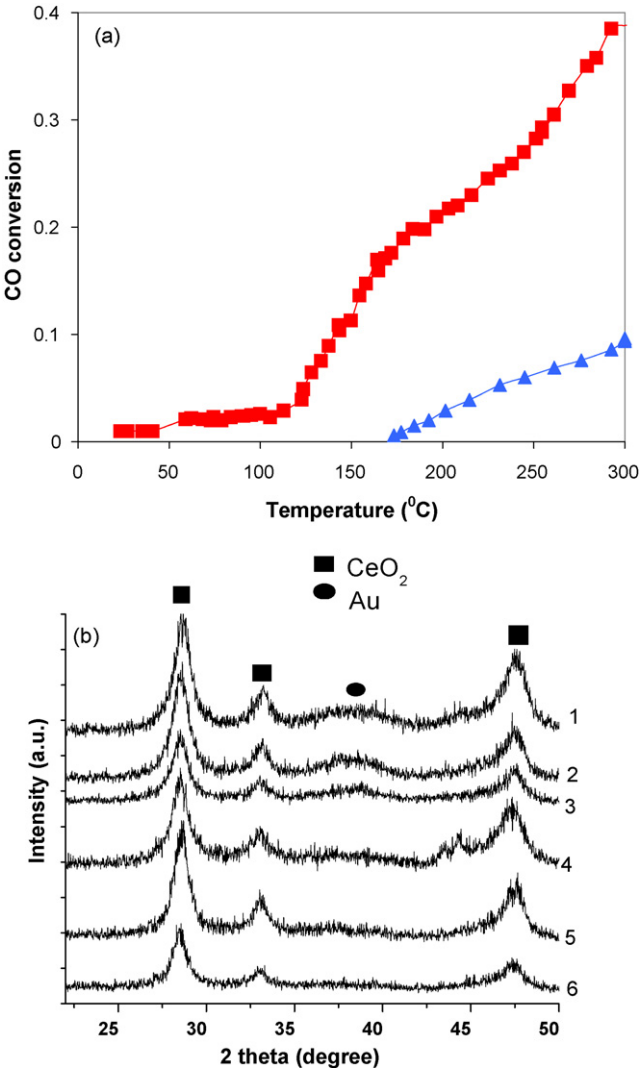

Fig. 4. (a) CO oxidation in the absence of O_2 over $Au/CeO_x/Al_2O_3$ (■) and CeO_x/Al_2O_3 (▲) during co-feeding of 30 ml min^{-1} CO + Ar. (b) XRD patterns of $Au/CeO_x/Al_2O_3$ fresh (1) and used (2) (CO + O_2), (CO + Ar) (3), CeO_x/Al_2O_3 fresh (4), and used (CO + O_2) (5), (6) (CO + Ar). The square symbols correspond to CeO_2 and the circle symbols correspond to Au.

corresponding supports, the conversion of CO to CO_2 was 40% over $Au/CeO_x/Al_2O_3$ (300 °C) [50] (see Fig. 4a). Au/Al_2O_3 and γ-Al_2O_3 did not show any CO conversion, as expected, since there is no available oxygen, at least at temperatures below 300 °C. CeO_x/Al_2O_3 gave only 8% conversion at 300 °C.

XRD of the fresh and spent $Au/CeO_x/Al_2O_3$ catalysts (Fig. 4b) showed no significant change in the structure of both Au and ceria. For comparison, the same figure displays the XRD results for the samples after CO oxidation. The structure of ceria for the fresh samples corresponds to CeO_2 (Ce^{4+}) and the same structure was found for the spent samples. Thus, although CO_2 could be formed in the absence of O_2, there is no noticeable reduction of Ce^{4+} to Ce^{3+}. These results suggest that only the near surface oxygen atoms, known as highly mobile species, play an active role in the CO oxidation and the temperature and reaction conditions used are not sufficiently high to reduce CeO_2 into Ce_2O_3.

Concerning the catalytic performance displayed by the multicomponent Au-based catalysts, the role of alkali (earth) metal oxides prevails over that of ceria, at least in the low temperature regime, where very small Au particles are more important. At temperatures above 120 °C, the active oxygen may also originate from ceria. It is possible that various pathways are active simultaneously, eventually in direct relationship with reaction temperature and/or other experimental factors such as moisture, flow rate, etc.

A relevant question is how the alkali (earth) oxides act as structural promoters, viz. why the gold particle size remains small in the presence of these promoters. The characterization methods used in this study did not point to an effect of the promoter on the nature of the relevant species: only metallic Au and CeO_2 have been detected. It is known from the solid state literature that Au, alkali (earth) metals and cerium or aluminium can form stable mixed oxides [51,52]. Therefore, we suggest that during preparation of the promoted catalyst a mixed Au, alkali earth, Ce/Al oxide is formed at the interface of the metallic gold particles and the support. This mixed oxide layer with a concentration smaller than needed for detection with our techniques may act as a kind of glue for the gold nanoparticles and sintering is prevented.

5. Conclusions

Unpromoted Au/Al_2O_3 catalysts are active in low-temperature CO oxidation. Important promoting effects are obtained by using additives such as alkali (earth) metal oxides. Their role is primarily related to stabilizing the very small gold particles, which are highly active towards activation of molecules. The largest promoting effect is found upon addition of BaO and full conversion of CO is already obtained at room temperature. In spite of the well-known promoting effect of ceria for various oxidation reactions, its addition to Au/Al_2O_3 is rather detrimental under these reaction conditions. However, if BaO and CeO_x are both added to Au/Al_2O_3, the multicomponent catalyst resembles the catalytic behaviour of $Au/BaO/Al_2O_3$. It is suggested that CO is activated on Au and at the Au–support interface. The alkali (earth) metal oxides additives act as structural promoters and possibly also help in O_2 activation. If a reducible metal oxide is used as additive, the activation of O_2 is facilitated, especially above 120 °C.

Acknowledgement

The Netherlands Organization for Scientific research, NWO (Grant NWO/CW 99037 and NWO #047.015.003) is gratefully acknowledged for financial support.

References

[1] M. Haruta, T. Kobayashi, N. Yamada, Chem. Lett. 2 (1987) 405.
[2] D.T. Thompson, Gold Bull. 31 (1998) 111.
[3] D.T. Thompson, Gold Bull. 32 (1999) 12.
[4] M. Valden, X. Lai, D.W. Goodman, Science 281 (1998) 1647.
[5] G.C. Bond, Gold Bull. 34 (2001) 117.
[6] G.C. Bond, D.T. Thompson, Catal. Rev. Sci. Eng. 41 (1999) 319.
[7] G.C. Bond, D.T. Thompson, Gold Bull. 33 (2000) 41.
[8] M. Haruta, CATTECH 6 (2002) 102.
[9] M. Haruta, Gold Bull. 37 (2004) 27.
[10] M. Haruta, M. Date, Appl. Catal. A 222 (2001) 427.
[11] G.J. Hutchings, Gold Bull. 37 (2004) 3.
[12] G. Pattrick, E. van der Lingen, C.W. Corti, R.J. Holliday, D.T. Thompson, Top. Catal. 30/31 (2004) 273.
[13] R. Meyer, C. Lemire, S.K. Shaikhutdinov, H.-J. Freund, Gold Bull. 37 (2004) 72.
[14] G.C. Bond, C. Louis, D.T. Thompson, Catalysis by gold, Sci. Series, vol. 6, Imp. College Press, 2006.
[15] S.A.C. Carabineiro, D.T. Thompson, Catalytic applications for gold nanotechnology, in: Nanocatalysis, Springer, 2007, p. 377.
[16] M. Haruta, S. Tsubota, T. Kobayashi, H. Kageyama, M.J. Genet, B. Delmon, J. Catal. 144 (1993) 175.
[17] S.D. Lin, M. Bollinger, M.A. Vannice, Catal. Lett. 17 (1993) 245.
[18] R.J.H. Grisel, Supported gold catalysts for environmental applications, Ph.D. Thesis, Leiden University, 2002.
[19] M. Bollinger, M.A. Vannice, Appl. Catal. B 8 (1996) 417.
[20] F. Boccuzzi, A. Chiorino, M. Manzoli, P. Lu, T. Akita, S. Ichikawa, M. Haruta, J. Catal. 202 (2001) 256.
[21] R.J.H. Grisel, C.J. Weststrate, A. Goossens, M.W.J. Craje, A.M. van der Kraan, B.E. Nieuwenhuys, Catal. Today 72 (2002) 123.
[22] M. Mavrikakis, P. Stoltze, J.K. Norskov, Catal. Lett. 64 (2000) 101.
[23] N.A. Hodge, C.J. Kiely, R. Whyman, M.R.H. Siddiqui, G.J. Hutchings, Q.A. Pankhurst, F.E. Wagner, R.R. Rajaram, S.E. Golunski, Catal. Today 72 (2002) 133.
[24] C.K. Costello, M.C. Kung, S.-O. Oh, Y. Wang, H.H. Kung, Appl. Catal. A 232 (2002) 159.
[25] W.T. Wallace, R.L. Whetten, J. Am. Chem. Soc. 124 (2002) 7499.
[26] L.D. Socaciu, J. Hagen, T.M. Bernhardt, L. Woste, U. Heiz, H. Hakkinen, U. Landman, J. Am. Chem. Soc. 125 (2003) 10437.
[27] H. Hakkinen, U. Landman, J. Am. Chem. Soc. 123 (2001) 9704.
[28] A. Sanchez, S. Abbet, U. Heiz, W.-D. Schneider, H. Hakkinen, R.N. Barnett, U. Landman, J. Phys. Chem. A 103 (1999) 9573.
[29] S. Tsubota, M. Haruta, T. Kobayashi, A. Ueda, Y. Nakahara, Preparation of Catalysts V, Elsevier, 1991, p. 695.
[30] A.C. Gluhoi, B.E. Nieuwenhuys, Catal. Today 119 (2007) 305.
[31] A.C. Gluhoi, N. Bogdanchikova, B.E. Nieuwenhuys, J. Catal. 232 (2005) 96.
[32] A.C. Gluhoi, X. Tang, P. Marginean, B.E. Nieuwenhuys, Top. Catal. 39 (2006) 101.
[33] S.D. Lin, A.C. Gluhoi, B.E. Nieuwenhuys, Catal. Today 90 (2004) 3.
[34] A.C. Gluhoi, M.A.P. Dekkers, B.E. Nieuwenhuys, J. Catal. 219 (2003) 197.
[35] A.C. Gluhoi, N. Bogdanchikova, B.E. Nieuwenhuys, J. Catal. 229 (2005) 154.
[36] A.C. Gluhoi, Fundamental studies focused on understanding of gold catalysis, Ph.D. Thesis, Leiden University, Leiden 2005. ISBN: 90-9019950-0.
[37] A. Trovarelli, Catalysis by Ceria and Related Materials, Imperial College Press, London, 2002.
[38] F. Boccuzzi, A. Chiorino, S. Tsubota, M. Haruta, Catal. Lett. 29 (1994) 225.
[39] I.N. Remediakis, N. Lopez, J.K. Norskov, Angew. Chem. Int. Ed. 44 (2005) 1824.
[40] G.R. Bamwenda, S. Tsubota, T. Nakamura, M. Haruta, Catal. Lett. 44 (1997) 83.
[41] F. Boccuzzi, A. Chiorino, S. Tsubota, M. Haruta, J. Phys. Chem. B 100 (1996) 3625.
[42] N. Lopez, T.V.W. Janssens, B.S. Clausen, Y. Xu, M. Mavrikakis, T. Bligaard, J.K. Norskov, J. Catal. 223 (2004) 232.
[43] N. Lopez, J.K. Norskov, T.V.W. Janssens, A. Carlsson, A. Puig-Molina, B.S. Clausen, J.D. Grunwaldt, J. Catal. 225 (2004) 86.
[44] B.E. Nieuwenhuys, A.C. Gluhoi, E.D.L. Rienks, C.J. Weststrate, C.P. Vinod, Catal. Today 100 (2005) 49.
[45] Z.-P. Liu, P. Hu, A. Alavi, J. Am. Chem. Soc. 124 (2002) 14770.
[46] G.B. Hoflund, S.D. Gardner, D.R. Schryer, B.T. Upchurch, E.J. Kielin, Appl. Catal. B 1995 (1995) 117.

[47] P. Bera, M.S. Hegde, Catal. Lett. 79 (2002) 75.
[48] M.P. Casaletto, A. Longo, A.M. Venezia, A. Martorana, A. Prestianni, Appl. Catal. A 302 (2006) 309.
[49] S. Carrettin, P. Concepcion, A. Corma, J.M. Lopez Nieto, V.F. Puentes, Angew. Chem. Int. Ed. (2004) 2538.
[50] A.C. Gluhoi, H.S. Vreeburg, J.W. Bakker, B.E. Nieuwenhuys, Appl. Catal. A 291 (2005) 145.
[51] H.D.v. Wasel-Nielen, R. Hoppe, Zeit. Anorg. Algem. Chem. 375 (1970) 43.
[52] J.-F. Brice, A. Ramdani, Mater. Res. Bull. 16 (1981) 1487.